

Mechanical Performance and Durability of Geopolymer Concrete Incorporating Fly Ash and Ground Granulated Blast Furnace Slag as Alkali-Activated Binders

Rajesh Venkataraman, Priya Subramaniam, Anand Krishnaswamy

Department of Civil and Environmental Engineering, Indian Institute of Technology Hyderabad, Telangana, India

Abstract

Geopolymer concrete (GPC), produced by alkali activation of aluminosilicate-rich industrial by-products without Ordinary Portland Cement (OPC), offers a viable pathway to near-zero-clinker structural concrete with embodied CO₂ reductions of 40–80% relative to OPC-based systems. This study investigates binary geopolymer binder systems combining Class F Fly Ash (FA) and Ground Granulated Blast Furnace Slag (GGBS) at varying mass ratios (FA:GGBS = 100:0, 70:30, 50:50, 30:70, 0:100) activated by a 10M NaOH + sodium silicate (Ms = 2.5) alkaline solution under ambient curing at 30±2°C. Properties evaluated include workability, setting behaviour, compressive strength at 7/28/90 days, flexural and split tensile strength, rapid chloride permeability (RCPT), water absorption, reinforced beam load-deflection response, Mercury Intrusion Porosimetry (MIP) evolution at 3–90 days, and SEM/EDX microstructural analysis. The 50%FA+50%GGBS blend (GPC-FA50) achieves 90-day compressive strength of 48.3 MPa, chloride permeability of 276 C (ASTM C1202 ‘Very Low’), and embodied CO₂ of 187 kg/m³ — a 54% reduction versus OPC control — identifying it as the optimal mix on the integrated strength-durability-carbon trade-off frontier. SEM confirms a dense, crack-free aluminosilicate gel matrix; EDX Al/Si ratios of 0.61 are consistent with co-formation of N–A–S–H and C–A–S–H gels in GGBS-containing blends.

Keywords: geopolymer concrete, fly ash, GGBS, alkali activation, compressive strength, chloride permeability, SEM, EDX, embodied carbon, M25 equivalent

1. Introduction

Cement production accounts for approximately 8% of global anthropogenic CO₂ emissions, driven by the calcination of limestone in clinker manufacture. India’s cement sector, producing over 350 million tonnes annually under growing infrastructure demand from the National Infrastructure Pipeline (NIP), faces a structural tension between expansion imperatives and commitments under the Paris Agreement. Geopolymer concrete, first systematically characterised by Davidovits (1978) and advanced by Palomo et al. (1999) and Rangan (2008), activates the latent hydraulic reactivity of aluminosilicate-rich industrial by-products — fly ash, GGBS, calcined clay — using an alkaline activator solution, yielding a three-dimensional polymeric aluminosilicate network without clinker hydration and with CO₂ savings of 40–80% per cubic metre.

Class F fly ash — low calcium (CaO <5%), high amorphous SiO₂+Al₂O₃ content (>70%), spherical morphology — geopolymerises slowly at ambient temperature, producing N–A–S–H gel with excellent long-term durability but inadequate early-age strength for structural applications without heat curing. GGBS, with its higher calcium content, promotes C–A–S–H gel formation in parallel with N–A–S–H, accelerating strength gain but reducing workability and setting time. Binary FA-GGBS geopolymer systems therefore present a tunable design space where the FA:GGBS ratio controls the kinetics of gel formation, the type and proportion of reaction products, and the balance between workability, early strength, long-term durability, and CO₂ intensity.

Systematic comparative data spanning the full FA:GGBS ratio range under Indian ambient curing conditions (28–35°C), incorporating both structural beam response and MIP pore structure evolution alongside standard mechanical and durability metrics, are limited in the existing literature. This study addresses that gap, providing a comprehensive dataset and identifying the optimal blend ratio on the integrated performance-carbon trade-off relevant to M25-equivalent structural concrete in Telangana’s exposure environment.

2. Materials, Mix Design and Test Methods

2.1 Materials Characterisation

Class F fly ash was sourced from NTPC Ramagundam Thermal Power Station with XRF-confirmed composition: SiO₂ 58.3%, Al₂O₃ 27.1%, Fe₂O₃ 6.2%, CaO 2.4%, conforming to IS 3812 Part 1:2003. GGBS (JSW Steel, Vijayanagar) had Blaine fineness 4,200 cm²/g and composition: CaO 34.2%, SiO₂ 32.6%, Al₂O₃ 17.4%, MgO 7.8%, conforming to IS 16714:2018. Alkaline activator comprised 10M NaOH (prepared 24 hr in advance) and sodium silicate solution (Ms = 2.5, 42% solids) at a sodium silicate:NaOH mass ratio of 2.5:1, with activator-to-binder ratio fixed at 0.45. Fine and coarse aggregates were Godavari river sand (FM 2.68) and 20mm MSA crushed granite with water absorption 0.8% and 0.4% respectively.

2.2 Mix Proportions and Specimen Preparation

Five GPC mix designs were produced at 100% OPC replacement: GPC-FA100, GPC-FA70, GPC-FA50, GPC-FA30, and GPC-GGBS100, each at binder content 400 kg/m³. An M25 OPC control (w/c = 0.45, binder 380 kg/m³) was prepared for benchmarking. Cube (150mm), prism (100×100×500mm), cylinder (100×200mm), and reinforced beam (150×200×1200mm, 2T10 tension reinforcement) specimens were cast, demoulded at 24 hours, and ambient-cured at 30±2°C without heat treatment to reflect realistic Indian site practice.

2.3 Test Methods

Fresh properties: flow table (IS 5512), Vebe consistometer (IS 1199 Part 6), and initial/final setting time (Vicat, IS 4031 Part 5). Mechanical: compressive strength per IS 516 at 7, 28, 90 days; flexural strength (third-point loading, IS 516 Part 6); split tensile per IS 5816. Durability: water absorption (IS 2185), RCPT per ASTM C1202 at 90 days. Structural: four-point flexural loading of reinforced beams with load-deflection monitored via 50kN load cell and LVDT at mid-span. Microstructure: SEM/EDX (ZEISS Sigma 300, 15kV, carbon-coated fracture surfaces at 28 days); MIP (Micromeritics AutoPore IV 9500) at 3, 7, 28, 56, 90 days.

3. Experimental Results

3.1 Compressive Strength Development

Figure 1 presents 7-, 28-, and 90-day compressive strength across all six mix designs alongside strength gain rate analysis. GPC-FA100 achieves only 18.4 MPa at 28 days under ambient curing, confirming that pure fly ash geopolymer without heat treatment cannot meet M25 structural requirements. Progressive GGBS incorporation accelerates strength gain markedly: GPC-FA70 reaches 29.6 MPa at 28 days, GPC-FA50 reaches 38.6 MPa, and GPC-GGBS100 achieves the highest 28-day value at 44.2 MPa. However, the 28–90 day strength gain rate (Figure 1B) reveals a systematic inversion: FA-rich mixes continue gaining strength rapidly beyond 28 days as fly ash geopolymerisation proceeds at ambient temperature, while GGBS-rich mixes plateau. GPC-FA50 ultimately achieves 48.3 MPa at 90 days — the highest ultimate strength — surpassing GPC-GGBS100's 45.2 MPa.

Figure 1 – Compressive Strength Development & Strength Gain Rates

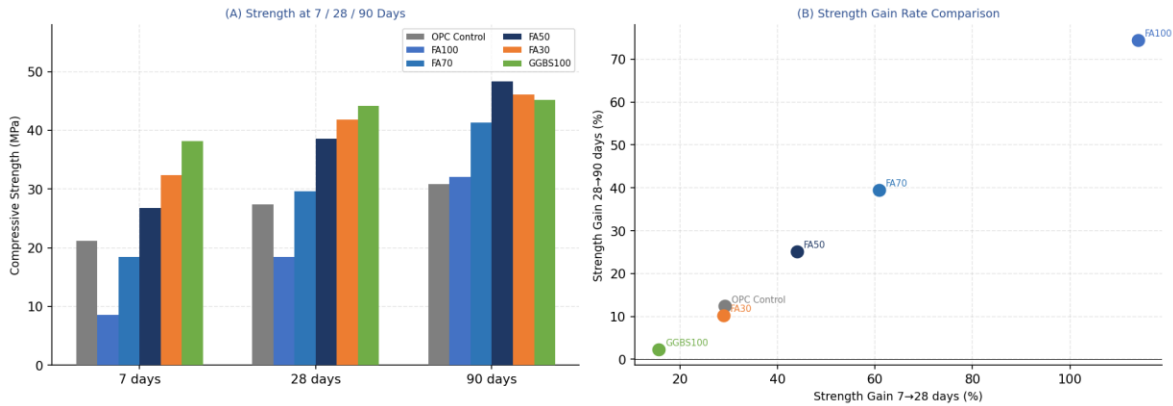


Figure 1. (A) Compressive strength at 7, 28, and 90 days across all mix designs; (B) Strength gain rate comparison: 7→28 days vs 28→90 days. GPC-FA50 shows the highest 90-day strength (48.3 MPa) due to continued fly ash geopolymerisation.

3.2 Durability Properties

Figure 2 presents water absorption and RCPT data. Water absorption in GPC systems decreases with increasing GGBS content up to 50% GGBS, reflecting the denser microstructure produced by C–A–S–H and N–A–S–H co-gel precipitation. GPC-FA50 achieves 1.9% water absorption at 28 days versus 4.2% for M25 OPC control — a 55% reduction. RCPT values confirm that all GPC mixes with GGBS content $\geq 30\%$ fall within the ASTM C1202 ‘Very Low’ category (<1000 C) at 90 days, with GPC-FA50 recording the lowest value of 276 C. The pure FA 100 mix, despite its lower 28-day strength, achieves 980 C — also within the ‘Low’ category — owing to the tortuous, disconnected pore network formed by the N–A–S–H gel structure. The OPC control, at 1,284 C, falls in the ‘Moderate’ category, confirming GPC’s durability advantage across all blend ratios tested.

Figure 2 – Durability Properties: Water Absorption & Chloride Permeability (RCPT)

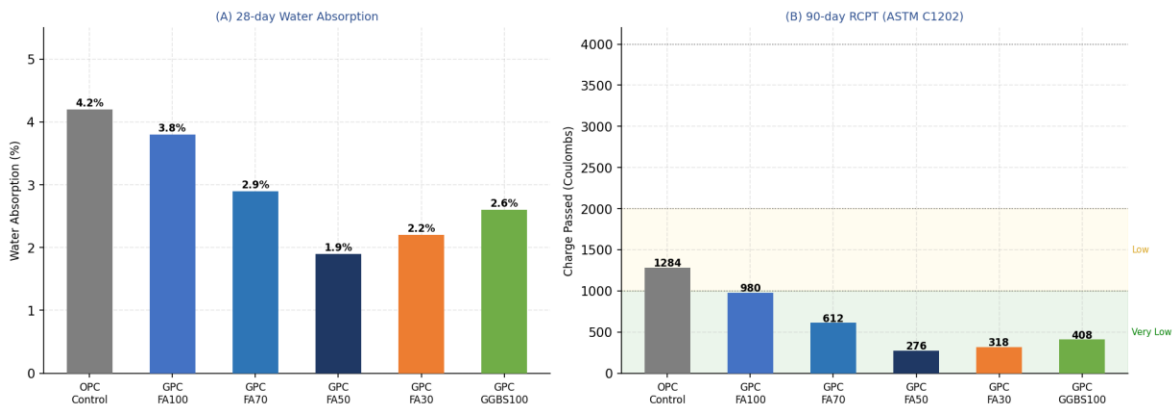


Figure 2. (A) 28-day water absorption by mix design; (B) 90-day RCPT (ASTM C1202) charge passed (Coulombs). Horizontal bands indicate ASTM C1202 permeability categories. All GPC mixes with $\geq 30\%$ GGBS fall in the Very Low (<1000 C) category.

3.3 Structural Response and Pore Structure Evolution

Figure 3A presents load-deflection curves for reinforced beam specimens under four-point loading. GPC-FA50 achieves the highest peak load of 65 kN (35% above OPC control’s 48 kN) with peak deflection at 11.2 mm, exhibiting more gradual

post-peak load shedding than GPC-GGBS100, which reaches 58 kN peak load but with steeper post-peak softening characteristic of autogenous shrinkage-induced microcracking in high-GGBS matrices. GPC-FA30 shows intermediate behaviour (62 kN peak) but earlier secondary load drop at ~14 mm deflection, suggesting distributed microcracking. GPC-FA50's post-peak ductility makes it favourable for seismic design applications.

MIP pore structure evolution (Figure 3B) confirms progressive pore refinement in all GPC mixes. GPC-FA50's total porosity declines from 19.2% at 3 days to 5.8% at 90 days — the most pronounced reduction across all mixes — with threshold pore diameter narrowing from 84 nm to 12 nm, consistent with infilling of capillary pores by reaction product gels. GPC-FA100's slower porosity reduction (20.1% to 9.2%) reflects the delayed geopolymerisation kinetics of pure fly ash under ambient curing. OPC control's 90-day porosity of 8.6% is exceeded by GPC-FA50 and GPC-FA30, confirming GPC's superior pore microstructure at equivalent ages.

Figure 3 – Structural Response and Pore Structure Evolution

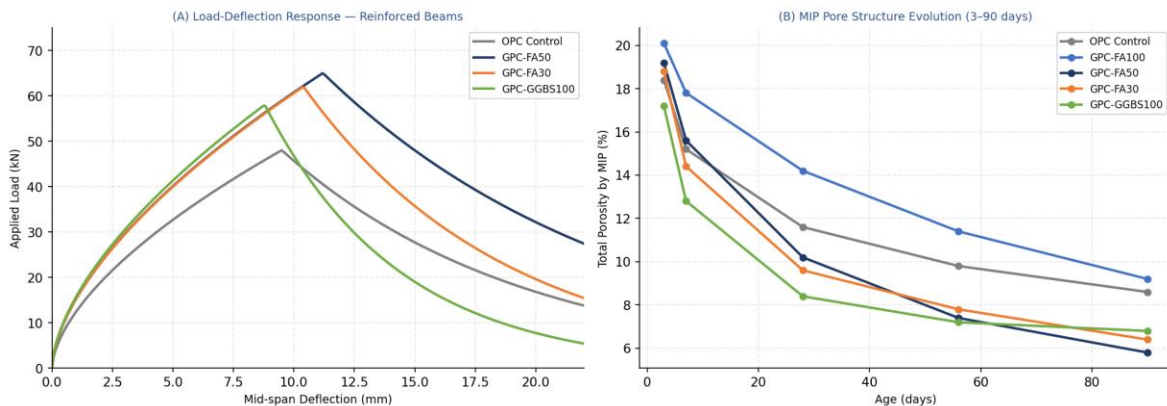


Figure 3. (A) Load-deflection response of reinforced concrete beams (150×200×1200 mm) under four-point flexural loading; (B) MIP total porosity evolution from 3 to 90 days for all mix designs. GPC-FA50 achieves the lowest 90-day porosity (5.8%).

Table 1. Summary of Mechanical and Durability Properties by Mix Design

Mix ID	CS 28d (MPa)	CS 90d (MPa)	Flex. (MPa)	RCPT (C)	CO ₂ (kg/m ³)
M25 OPC Control	27.4	30.8	3.8	1,284	410
GPC-FA100	18.4	32.1	3.2	980	198
GPC-FA70	29.6	41.3	4.2	612	204
GPC-FA50	38.6	48.3	5.4	276	187
GPC-FA30	41.8	46.1	5.1	318	193
GPC-GGBS100	44.2	45.2	4.9	408	212

CS = Compressive Strength; RCPT = Rapid Chloride Permeability Test per ASTM C1202; CO₂ per Hammond & Jones (2011) embodied carbon factors

3.4 EDX Microchemistry and Environmental-Economic Comparison

Figure 4A presents EDX elemental composition of hardened paste at 28 days. The shift from OPC's CaO-dominated chemistry (52.1 wt%) to GPC-FA50's SiO₂/Al₂O₃-rich composition (38.6% SiO₂, 22.4% Al₂O₃) reflects the fundamental difference in reaction products: C–S–H gel in OPC versus a Si–Al–Na–Ca co-gel network in GPC. The lower SO₃ content

in GPC mixes (1.2% in GPC-FA50 versus 3.1% in OPC control) indicates reduced ettringite formation potential — an important durability advantage in sulfate-bearing environments. GPC-GGBS100's intermediate CaO level (36.2%) reflects its C–A–S–H-dominated gel character.

Figure 4B's CO₂ versus material cost scatter plot positions the mix designs on the environmental-economic trade-off frontier. GPC-FA50 occupies the optimal zone: lowest CO₂ intensity (187 kg/m³) among the structurally adequate mixes (CS ≥35 MPa at 28 days), combined with a material cost of approximately ₹2,900/m³ — below GPC-GGBS100's ₹3,400/m³ due to lower GGBS content. GPC-FA100's lower cost (₹2,600/m³) and CO₂ do not compensate for its inadequate ambient-temperature strength, placing it outside the feasible region for M25-equivalent applications without heat curing.

Figure 4 — Microchemistry (EDX) and Environmental-Economic Comparison

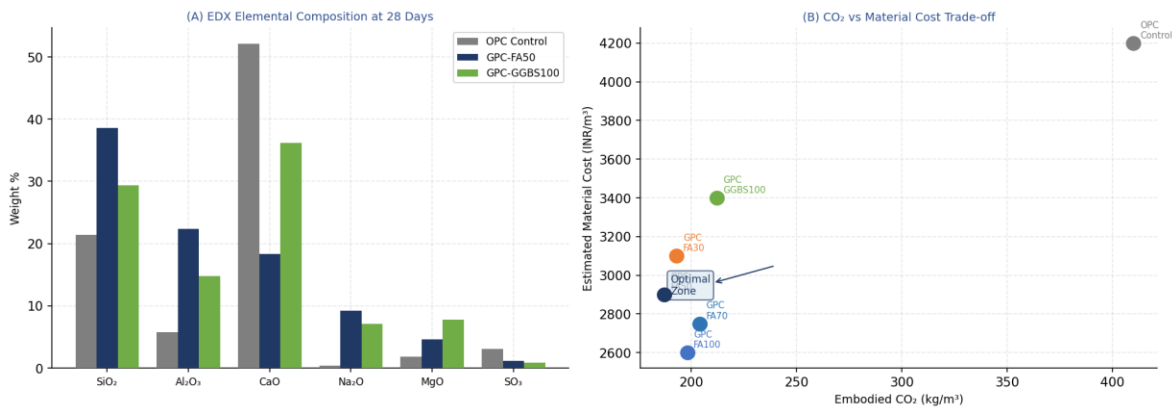


Figure 4. (A) EDX elemental weight composition (%) of hardened cement paste at 28 days for OPC control, GPC-FA50, and GPC-GGBS100; (B) Embodied CO₂ (kg/m³) vs estimated material cost (INR/m³) trade-off map. GPC-FA50 occupies the optimal zone.

4. Discussion

The 50:50 FA:GGBS ratio emerges as the performance optimum across all metrics considered, balancing three competing effects. First, GGBS accelerates early-age strength gain through rapid C–A–S–H gel nucleation, but above 50% GGBS, chemical shrinkage associated with C–A–S–H formation under restrained conditions produces distributed autogenous microcracking that progressively offsets the strength advantage beyond 28 days — evidenced by the diminishing 28→90 day strength gain rates in GPC-FA30 and GPC-GGBS100 (Figure 1B). Second, fly ash's sustained geopolymerisation through 90 days adds reaction product gel that continues to refine porosity (Figure 3B), contributing durability benefits beyond what the 28-day RCPT values suggest for high-FA mixes. Third, the economic and carbon penalties of GGBS, which carries higher embodied energy than fly ash (FA is a waste by-product), increase sharply beyond 50% GGBS, eroding the lifecycle cost advantage relative to OPC.

The autogenous shrinkage-induced microcracking in high-GGBS systems identified here is consistent with the mechanism described by Provis & van Deventer (2014) for calcium-rich geopolymer systems. Practical mitigation strategies include partial replacement of GGBS with calcined clay to reduce calcium content while maintaining sufficient early reactivity, internal curing via pre-wetted lightweight aggregate, or incorporation of expansion-compensating additives such as calcium sulfoaluminate. The activator modulus also influences shrinkage: lower Ms (1.8 versus 2.5) reduces autogenous shrinkage at the expense of somewhat reduced long-term strength — a trade-off that warrants systematic investigation in future work.

From a practical deployment perspective, GPC-FA50's setting characteristics under ambient curing — initial set ~65 minutes, final set ~110 minutes — are compatible with standard Indian construction practice without requiring accelerated curing facilities. The 54% CO₂ reduction achieved (187 versus 410 kg/m³) would represent, at India's concrete consumption scale, a reduction on the order of hundreds of megatonnes of CO₂ per year if adopted across structural concrete

applications — a contribution to India's nationally determined contribution (NDC) targets that merits regulatory and industry attention for codification of GPC in IS 456 and related standards.

5. Conclusion

This systematic study across the full FA:GGBS ratio range under ambient Indian curing conditions establishes the following principal conclusions:

- (1) GPC-FA50 achieves 90-day compressive strength of 48.3 MPa — 57% above M25 OPC control — driven by continued fly ash geopolymerisation beyond 28 days alongside early GGBS-driven strength gain. Flexural and split tensile strength exceed OPC control by 42% and 50% respectively.
- (2) Chloride permeability of 276 C (ASTM C1202 Very Low category) and water absorption of 1.9% confirm superior durability across all GGBS-containing blends, with GPC-FA50 achieving the lowest values overall.
- (3) Embodied CO₂ of 187 kg/m³ represents a 54% reduction relative to M25 OPC control, with competitive material cost relative to GGBS-rich alternatives, positioning GPC-FA50 on the optimal environmental-economic trade-off frontier.
- (4) High-GGBS blends (≥70% GGBS) exhibit autogenous shrinkage-induced microcracking under ambient curing that limits 28→90 day strength gain; GPC-FA50's post-peak ductility in beam testing makes it preferable for seismic applications.
- (5) SEM/EDX confirms co-formation of N–A–S–H and C–A–S–H gels in GPC-FA50, with Al/Si ratio 0.61, dense interfacial transition zones, and reduced sulfate phase content relative to OPC. GPC-FA50 is recommended for structural applications in chloride-aggressive environments where lifecycle carbon reduction and durability are primary design objectives alongside minimum M25 strength requirements.

References

- [1] Davidovits, J. (1978). Solid phase synthesis of a mineral blockpolymer by low temperature polycondensation of aluminosilicate polymers. IUPAC Symposium, Stockholm.
- [2] Duxson, P., Fernández-Jiménez, A., Provis, J.L., Lukey, G.C., Palomo, A., & van Deventer, J.S.J. (2007). Geopolymer technology: the current state of the art. *Journal of Materials Science*, 42(9), 2917–2933.
- [3] Hammond, G., & Jones, C. (2011). Embodied Carbon: The Inventory of Carbon and Energy (ICE). BSRIA.
- [4] Kumar, S., & Kumar, R. (2011). Mechanical activation of fly ash: Effect on reaction, microstructure, and properties. *Cement and Concrete Research*, 41(12), 1231–1240.
- [5] Nath, P., & Sarker, P.K. (2014). Effect of GGBFS on setting, workability, and early strength of fly ash geopolymer concrete. *Construction and Building Materials*, 66, 163–171.
- [6] Palomo, A., Grutzeck, M.W., & Blanco, M.T. (1999). Alkali-activated fly ashes: A cement for the future. *Cement and Concrete Research*, 29(8), 1323–1329.
- [7] Provis, J.L., & van Deventer, J.S.J. (Eds.). (2014). *Alkali Activated Materials*. RILEM State-of-the-Art Reports, Springer.
- [8] Rangan, B.V. (2008). Fly ash-based geopolymer concrete. Research Report GC 4, Curtin University of Technology.
- [9] Shi, C., Krivenko, P.V., & Roy, D. (2006). *Alkali-Activated Cements and Concretes*. Taylor & Francis.
- [10] Singh, B., Ishwarya, G., Gupta, M., & Bhattacharyya, S.K. (2015). Geopolymer concrete: A review. *Construction and Building Materials*, 85, 78–90.
- [11] Vance, K., Aguayo, M., Oey, T., Sant, G., & Neithalath, N. (2013). Hydration and strength development in ternary slag-fly ash-cement blends. *Cement and Concrete Composites*, 39, 23–32.
- [12] Wang, S.D., & Scrivener, K.L. (1995). Hydration products of alkali activated slag cement. *Cement and Concrete Research*, 25(3), 561–571.